TITLE
In vivo knee contact force prediction using patient-specific musculoskeletal geometry in a segment-based computational model

AUTHOR
Ding, Ziyun; Nolte, Daniel; Kit Tsang, Chui; et al.

JOURNAL
Journal of Biomechanical Engineering

DATE DEPOSITED
29 April 2016

In Vivo Knee Contact Force Prediction Using Patient-Specific Musculoskeletal Geometry in a Segment-Based Computational Model

In Vivo Knee Contact Force Prediction Using Patient-Specific Musculoskeletal Geometry in a Segment-Based Computational Model

Ding, Ziyun
Department of Bioengineering
Imperial College London
London, SW7 2AZ United Kingdom
z.ding@imperial.ac.uk

Nolte, Daniel
Department of Bioengineering
Imperial College London
London, SW7 2AZ United Kingdom
d.nolte@imperial.ac.uk

Tsang, Chui Kit
Department of Bioengineering
Imperial College London
London, SW7 2AZ United Kingdom
chui.k.tsang@gmail.com

Cleather, Daniel J
School of Sport, Health and Applied Science
St Mary's University
Waldegrave Road, Twickenham, TW1 4SX United Kingdom
daniel.cleather@stmarys.ac.uk

Kedgley, Angela E[1]
Department of Bioengineering
Imperial College London
London, SW7 2AZ United Kingdom
akedgley@imperial.ac.uk

Bull, Anthony M J
Department of Bioengineering
Imperial College London
London, SW7 2AZ United Kingdom
a.bull@imperial.ac.uk

[1] Corresponding author.

ABSTRACT

Segment-based musculoskeletal models allow the prediction of muscle, ligament and joint forces without making assumptions regarding joint degrees of freedom. The dataset published for the "Grand Challenge Competition to Predict In Vivo Knee Loads" provides directly-measured tibiofemoral contact forces for activities of daily living. For the "Sixth Grand Challenge Competition to Predict In Vivo Knee Loads", blinded results for "smooth" and "bouncy" gait trials were predicted using a customised patient-specific musculoskeletal model. For an unblinded comparison the following modifications were made to improve the predictions:

- further customisations, including modifications to the knee centre of rotation;
- reductions to the maximum allowable muscle forces to represent known loss of strength in knee arthroplasty patients; and
- a kinematic constraint to the hip joint to address the sensitivity of the segment-based approach to motion tracking artefact.

For validation, the improved model was applied to normal gait, squat and sit-to-stand for three subjects. Comparisons of the predictions with measured contact forces showed that segment-based musculoskeletal models using patient-specific input data can estimate tibiofemoral contact forces with root mean square errors (RMSEs) of 0.48-0.65 times body weight (BW) for normal gait trials. Comparisons between measured and predicted tibiofemoral contact forces yielded an average coefficient of determination of 0.81 and RMSEs of 0.46-1.01 times BW for squatting and 0.70-0.99 times BW for sit-to-

stand tasks. This is comparable to the best validations in the literature using alternative models.

INTRODUCTION

An important mechanical function of the musculoskeletal system is to actuate and provide motion and, as such, transmit the forces associated with that motion. These forces induce stresses and deformations in multiple tissues, including the muscles, articular surfaces, and ligaments. Musculoskeletal models allow the mechanical function of the musculoskeletal system to be quantified and analysed. Validation of the outputs of musculoskeletal models using in vivo measures is possible through comparison with a range of measurements, including electrical activity within the muscles [1], tendon forces [2], and articular contact force via instrumented implants [3]. As muscle forces directly produce articular contact forces, instrumented implants provide not only explicit validation of these contact forces, but also indirect validation of the muscle forces that produce the contact forces at the joints.

Musculoskeletal modelling is a technology that is now reaching maturity with multiple validation studies demonstrating that articular contact forces can be quantified with a high level of accuracy for gait [4-7] and shoulder motions [8]. However, to date there has been minimal validation for the wider activities of daily living (ADLs) [9,10]. Data now exist that will allow such a validation [11].

Most musculoskeletal models are posed in such a way as to assume a fixed centre of rotation for each joint [12], or a fixed or defined path of motion [13,14]. These, therefore, do not take into account any variations in the contact at the joint that may

occur as a result of the differing loading conditions during the performance of ADLs, in particular at the surfaces of a total knee joint replacement, the contact points of which move up to 36 mm [15].

Cleather and Bull have proposed a segment-based musculoskeletal model of the lower limb, allowing full six degrees of freedom movement of each lower limb segment with no joint constraints [16]. Given each segment's position in generalised coordinates [17], the model is capable of estimating muscle forces, ligament forces and articular contact forces acting upon the segment simultaneously [18]. Since the mechanical function of muscle elements, ligaments, and articular contact forces exerted upon the segments is explicitly described in the force equilibrium, the model can provide additional insights into the musculoligamentous interaction [18] and functional role of biarticular muscles [19]. However, previously only a generic musculoskeletal model was implemented and the estimated forces were not fully validated.

The aims of this study, which was undertaken in the framework given in the "Sixth Grand Challenge Competition to Predict In Vivo Knee Loads", are to: (1) customise a subject-specific segment-based musculoskeletal model and compare tibiofemoral outcomes for two different variations of gait; (2) assess the influence of personalized musculoskeletal geometry data, strength data, and appropriate kinematic constraint on tibiofemoral loading and (3) validate outcomes for other ADLs, namely 'normal' gait, rising from a chair, and squatting. For the first aim a set of blinded contact force predictions was generated without knowledge of the measured contact forces. After the contact force measurements were released as part of the competition, a set of

unblinded predictions was generated with some modifications to the model. Therefore, this paper comprises two parts: the first part presents methods, results and discussion for the unblinded predictions; the second part presents methods, results and discussion for the unblinded predictions, performing a wide validation based on the database of "Grand Challenge Competition to Predict In Vivo Knee Loads". A final conclusion section summarises both sets of predictions.

METHODS FOR BLINDED PREDICTIONS

Experimental Data

All experimental data used in this blinded study were obtained from the publically available database that was released as part of the sixth "Grand Challenge Competition to Predict In Vivo Knee Loads" [11]. The data for the blinded predictions were obtained from a single male subject (DM, age: 83 years, height: 172 cm, mass: 70 kg) who had an instrumented Generation II tibial component (eTibia) implanted as part of a total knee replacement on the right knee [20]. Available data that were used included pre- and post-operative computed tomography (CT) scans, implant component and bone models of the implanted leg, optical motion capture data, and ground reaction forces.

Two variations of overground gait were analysed, "bouncy" and "smooth", which reflect different magnitudes of superior-inferior translation of the pelvis [21]. In bouncy gait this translation is higher than in smooth gait. The bouncy gait cycle came from the DM_bouncy5 trial and had a start time of 1.876 s and an end time of 3.075 s. The

smooth gait cycle came from the DM_smooth1 trial and had a start time of 2.53 s and an end time of 3.775 s.

Musculoskeletal Model

A custom-written three-dimensional musculoskeletal model of the lower limb, FreeBody [17], was used for this study. FreeBody is a publicly available musculoskeletal model of the lower limb (available at www.msksoftware.org.uk) that is packaged as a MATLAB (The Mathworks Inc., Natick, USA) application. It consists of five rigid segments – foot, shank, patella, thigh, and pelvis – articulated by four joints – ankle, tibiofemoral, patellofemoral joint, and hip. The computational approach adopted within the software is distinct from the majority of lower limb models described within the literature [7,12,22-24]. Firstly, the model is posed entirely on the basis of segmental motion, rather than considering joint motion. Captured marker trajectories directly define segmental motions. The segmental kinematic data and measured ground reaction forces are used in an inverse dynamic analysis. The inverse dynamic analysis is implemented using quaternion algebra and wrench notation to describe the kinematics [17,26]. Secondly, muscle forces, ligament forces and articular contact forces that act upon each segment and contribute to its motion are solved simultaneously in the optimisation stage, using an objective function minimising the sum of cubed muscle stresses [1]. A total of 22 equations of motion are constructed: 18 equations describing the motions of the foot, shank and thigh segment allowing six degrees of freedom for each segment; three equations describing three linear motions of the patella; and one equation

describing the ratio between the forces of the quadriceps muscles and the patella ligament [16]. On the shank segment, the tibiofemoral joint reaction force is compartmentalised into a medial and a lateral component by the definition of contact points of the two femoral condyles. The effect of medial and lateral contact forces on the segment's motion is hence explicitly described in the equations of motion. The muscle forces were constrained using upper bounds determined by multiplying published physiological cross-sectional areas of each muscle [27] by an assumed maximum muscle stress (31.39 N/cm^2) [28].

The subject's anatomical model consists of 164 line elements representing 38 different lower limb muscles and the patellar ligament following topology from the literature [27]. Muscle origin, via, and insertion points, along with anatomic landmarks, joint centres (defined as different points relative to the proximal and distal segments, free to move relative to each other), and contact points between the femur and tibial plateau were manually digitized from the CT scans provided using Mimics (v. 16.0, Materialise, Leuven, Belgium). For points on the foot and pelvis that were not visible on the CT scans, bones of subjects with similar anthropometry were registered to the images and the points were digitised on these registered surfaces. Cylindrical wrapping objects, as described by Klein Horsman et al. [27], were also defined from the CT scans to represent the underlying anatomical structure of the femoral condyles and superior pubic ramus of the pelvis.

Raw motion capture data and synchronised ground reaction force data were filtered using a fourth-order Butterworth low pass filter with a cut-off frequency of 4 Hz.

To match the anatomical model to the dynamic trials, motion capture data of a static trial with the subject in a neutral standing position was required. A static trial with the feet pointing forward (DM_staticfor1) was selected. The segment's local coordinate system was defined using anatomical marker data recorded in the trial, including marker data on the anterior/posterior superior iliac spine, medial/lateral femoral epicondyle, medial/lateral malleolus and the second metatarsal. Unfortunately, the trial was missing the marker on the medial femoral epicondyle. The marker's position in the static trial was therefore reconstructed using the average of the point determined using two prediction methods which both minimised the distance between the tibial plateau and femoral epicondyles. In the first method, the segments from a second static trial (DM_staticout2) were aligned to the chosen neutral trial using the algorithm described by Söderkvist et al. [29]. In the second method, the positions of the thigh markers were calculated by minimising discrepancies between the relative positions of the hip centre of rotation, patellar marker, and femoral epicondyle positions obtained from the frame within the bouncy gait dynamic trial in which the leg was most straight. Furthermore, the anatomical landmark of the second metatarsal in the anatomical model was re-estimated in order to accommodate the right toe marker on the shoe in the static and dynamic trials.

Model Evaluation

Medial, lateral, and total tibiofemoral articular contact forces were calculated. Results were interpolated using cubic splines and resampled so values could be reported

in 1% increments over the gait cycle. Differences between the results from FreeBody and the experimental measurements were quantified by the root mean squared error (RMSE) and the coefficient of determination (R^2).

RESULTS FOR BLINDED PREDICTIONS

Tibiofemoral contact force magnitudes during smooth and bouncy gait for medial, lateral, and total tibiofemoral contact forces were calculated (Fig. 1). RMSE and R^2 values when compared to directly measured data are listed in Table 1. In both gait variations the R^2 value of the total error is higher than that on either side separately. Smaller total errors were found in the lateral compartment, with RMSE values of 0.46 and 0.27 times body weight (BW) for smooth and bouncy gait, respectively. The RMSE values on the medial side were 0.56 and 0.60 times BW for smooth and bouncy gait, respectively. On the lateral side this was predominantly due to an overprediction of the second peak of the gait cycle, which reached 70% of the measured load in the smooth gait trial. Errors in the medial compartment were more consistent across the cycles. The RMSE of the total force was 0.77 and 0.62 times BW for smooth and bouncy gait respectively.

DISCUSSION OF BLINDED PREDICTIONS

Predicted forces consistently exceeded those measured in vivo with an RMSE of 0.69 times BW on average – as has been the case with other blinded predictions in the

literature. Previous models have predicted tibiofemoral contact forces with an RMSE of 0.69 [30], 0.66 [31], 0.67 [32] and 0.48 [33] times BW during gait. The timings of peak contact forces were correctly identified in both gait trials; however, the values of the peak contact forces were overpredicted with a maximum error of 0.66 times BW on the second peak of stance during gait. Other authors have reported errors in peak value estimation ranging between 0.35 and 0.80 times BW [7,31, 34-35].

The greater agreement, as quantified by the R^2 value, between measured and calculated total contact forces, when compared to those in either compartment separately, indicated that the distribution of the contact forces between the medial and lateral sides could be improved.

Muscle geometries were modelled as accurately as possible using manual digitisation of the CT scan in order to create the subject-specific anatomical model. Nevertheless, prediction results were also influenced by the reconstruction of the static marker data which was needed to map the dynamic kinematic data to the anatomical model. As the static trial was missing the medial femoral condyle marker, it was necessary to fit marker data from the bouncy gait trial to recreate the complete static dataset. Despite using rigid body registration [29], this procedure may still have introduced errors into the kinematic parameters. Calculation of inverse kinematics using a segment-based approach is sensitive to skin motion artefact [36] and therefore it is recommended that, in some cases, consideration is given to applying additional kinematic constraints. This is considered in the next section of this manuscript.

Muscle strengths were taken from a generic dataset based on the physiological cross sectional area (PCSA) [27]. As muscle strength reduces with age in ways that do not scale with PCSA [37] and do not scale for all muscles equally [38], the model could be improved through the incorporation of subject-specific strength measures that are likely to change the medio-lateral force distribution.

MODIFIED METHODS FOR UNBLINDED PREDICTIONS

Experimental Data

The modified model described below was tested on a series of three subjects (DM, PS, JW; age: 84 ± 1.7 years, height: 173 ± 6 cm, weight: 70.6 ± 4.2 kg) from the fourth through sixth "Grand Challenge Competition to Predict In Vivo Knee Loads" [11] for three ADLs: overground gait, sit-to-stand, and squatting. All three subjects had an instrumented total knee replacement; two subjects had the instrumented Generation II tibial component (eTibia) [20], while the third had an instrumented Generation I tibial component (eKnee) [39]. Once again, available data included CT scans, optical motion capture data, and ground reaction forces. Isometric strength data were available for two of the three subjects.

Kinematic data for gait trials were extracted by manually selecting sequential heel strikes on the force plate from the available c3d files. For the sit-to-stand task, cycles started with the subject in an upright seated position just prior to the forward motion of the upper body that initiated the motion. Each cycle ended with the subject in an upright seated position, following a backward movement of the upper body. For the

squatting task, a cycle was defined between two upright standing positions; the start of the motion was characterised by the first bend of the knee from a neutral position and the end by the return to a static neutral position.

The number of available trials for each subject and each activity varied (DM: 3 gait, 3 sit-to-stand, 2 squatting; PS: 6 gait, 2 sit-to-stand, 4 squatting; JW: 5 gait, 4 sit-to-stand, 3 squatting); the mean results for each task were calculated at each percentage of the cycle.

Musculoskeletal Model

Several modifications were made to improve the predictions from the blinded results. These included the following customisations: modifications to the knee centre of rotation; the locations of markers in the static trial; and reduction of the maximum allowable muscle forces. Additionally, in order to address the sensitivity of the segment-based approach to motion tracking artefact, a kinematic constraint to the hip joint centre was applied.

The tibiofemoral joint centre, as originally determined from the CT scans, was located about 7 mm lateral, inferior and anterior to the mid-point of the femoral epicondyles as a centre of a sphere best approximating the curvature of the bone at the femoral condyles. However, subject DW's anteroposterior radiographs showed a valgus tibiofemoral alignment. This could also be observed in the static trial marker data, but could not be determined in the anatomical dataset due to image artefacts in the CT caused by the implant. The valgus angulation of 174° in the frontal plane was used to

alter the definitions of the anatomical dataset. Therefore, the knee centre was re-estimated in order to ensure correct leg alignment. Compared to the estimation of the knee centre used for the blinded results, the position was moved 13.6 mm toward the medial, proximal and posterior direction.

With the assistance of visualisation tools within FreeBody, marker data on the subject's shank and thigh collected during the static trial were further adjusted iteratively in order to better match their placements relative to those in the first frame of the gait trials. This resulted in a reduction in the discrepancy of marker placements between the static trial and the first frame of the gait trials from up to 5.2 mm to 1.5 mm.

It has been shown that the strength of both flexor and extensor muscles is reduced for patients following total knee arthroplasty [40]. When compared with a group of control subjects from the literature (age: 62±7.3 years; height: 168.8±11.6 cm; weight 82.4±18.3 kg; BMI: 28.9±5.9 kg/m^2) [40] isometric extension and flexion peak torques for DM were found to be 30.3% and 50.3% lower, respectively (Table 2). In order to represent the patient-specific reductions of muscle strength, coefficient factors were introduced into the cost function for the knee flexors and extensors

$$c_e \sum_{i\epsilon M_e} \left(\frac{f_i}{f_{imax}}\right)^3 + c_f \sum_{i\epsilon M_f} \left(\frac{f_i}{f_{imax}}\right)^3 + \sum_{i\epsilon M \setminus (M_e \cup M_f)} \left(\frac{f_i}{f_{imax}}\right)^3 \quad (1)$$

where f_i and f_{imax} are the muscle and maximal muscle force, respectively; c_e is the coefficient factor for the knee extensor; c_f is the coefficient factor for the knee flexors; M is the list of all muscles; M_e is the index for the knee extensors, which included rectus

femoris, vastus medialis, vastus laterals, and vastus intermedius; M_f is the index for the knee flexors, which included gastrocnemius, biceps femoris (long head), semitendinosus, semimembranosus, sartorius, gracilis, popliteus, and plantaris.

In the segment-based model, the positions and orientations of each segment were determined independently, based upon the trajectories of the markers on each. Modelled as a fixed point in the adjacent distal segment, each joint has full six degrees of freedom with respect to its proximal segment. However, for those subjects for which no joint translation is observed or possible, for example in patients with a fully-functioning hip arthroplasty, then constraining joint translation provides the opportunity to reduce kinematic measurement errors due to skin motion artefact. Therefore, a kinematic constraint was applied to the hip joint, retaining three rotational degrees of freedom only. This was used for the single subject who had hip joint arthroplasty.

In each subject-specific anatomical dataset, a local pelvic coordinate frame was constructed in terms of markers on anterior and posterior superior iliac spines. The hip centre of rotation, determined from the CT scan, was then transformed within this local frame. In order to model the hip joint arthroplasty of subject JW, a recipient of hip arthroplasty, the joint was restricted to have three rotational degrees of freedom; in each dynamic trial, the position of the thigh segment, as provided from the optical motion capture, was translated such that the femoral head was aligned with the hip centre within the pelvic frame.

Model Evaluation

All predicted results were rescaled to a time interval from 0 to 100% using cubic spline interpolation. Differences between the predicted forces and the experimental measurements over each cycle were evaluated by calculating the root mean squared error (RMSE) and the coefficient of determination (R^2). The peak values of articular contact forces were compared as a discrete assessment.

Further, linear envelopes of the EMG data were computed through high-pass filtering, rectification, lower-pass filtering and normalisation of the magnitude following the procedure described in Arnold et al. [41]. Predicted muscle forces of the blinded and unblinded models were compared with the linear envelopes using a threshold method [42, 43]: a muscle is defined as active if the mean EMG value is above 20% of the maximal EMG envelope for the period of one of the seven gait phases described in Giroux et al. [42].

RESULTS FOR UNBLINDED PREDICTIONS

Tibiofemoral contact force magnitudes during smooth and bouncy gait for medial, lateral, and total tibiofemoral contact forces were calculated using the modified model (Fig. 2). In comparison with the blinded results, predicted values for both compartments decreased resulting in an improvement in RMSE and R^2 values (Table 3), particularly for the bouncy gait trial.

A good agreement with the muscle active/inactive states was found for predicted muscle forces crossing the ankle (soleus and tibialis anterior), knee (semimembranosus, vastus medialis/laterial and gastrocnemius) and hip (adductor brevis, and gluteus maximus) (Fig. 3). Timing inconsistencies between the predicted muscle forces and the EMG signals were observed for several muscles, for example, rectus femoris and sartorius: the rectus femoris produced a peak force in the initial swing phase, differing from the corresponding inactive EMG state; the sartorius was seen to lag behind its EMG envelope as it reached the peak force at the swing phase.

After the adjustment of muscle strength for knee flexors and extensors, predicted muscle forces were lower, e.g., for semimembranosus and biceps femoris in the loading response phase (0-17% of stance), and gastrocnemius medialis, sartorius and gracilis between the mid-stance to the mid-swing phase. This decreased the resultant tibiofemoral articular contact forces in the corresponding phases, especially in the medial compartment (Fig.2).

Results for normal gait, squatting, and sit-to-stand trials are presented in Tables 4-5. For normal gait, the experimental measurements revealed a double-peak total force during the gait cycle. The model over-estimated or under-estimated the peak values; for the first peak the error was 0.41 times BW on average and for the second peak the error reached 1.82 times BW for subject JW. During the squatting cycle, the measured contact force was greater in leg flexion than leg extension. The model predicted the pattern well with an R^2 value of 0.83 on average but consistently over-estimated the force magnitudes. During the sit-to-stand cycle, there are two peaks

observed for the measured contact forces. The model showed a high accuracy in predicting the pattern with an average R^2 value of 0.80 but errors in predicting the peak values. On average, the greatest agreement between measured and predicted total forces was in normal gait with an average RMSE of 0.54 times BW; the greatest differences in peak forces were observed in the sit-to-stand task, with errors of up to 2 times BW for subject PS.

DISCUSSION OF UNBLINDED PREDICTIONS

The first aim of this study was to model two different variations of gait, based on publically available datasets provided by the "Grand Challenge Competition to Predict In Vivo Knee Loads". Available data included CT imaging, kinematic data, kinetic data and strength data, which were used to customise subject-specific input to a segment-based musculoskeletal model. This allowed the simultaneous prediction of articular contact and muscle forces. Subject-specific anatomical geometry was constructed based on manual digitization of CT scans, and muscle strength was obtained based on measurement of maximal knee joint torques. A three-dimensional lower limb musculoskeletal model [16] was updated by implementing the subject-specific instantiation of anatomical data. For unblinded prediction an average R^2 value of 0.65 was obtained; however, the force magnitudes were overestimated with an average RMSE of 0.35 times BW.

The second aim of this study was to assess the influence of customised musculoskeletal input data on tibiofemoral loading, including the geometry data,

strength data and appropriate kinematic constraint. The most significant improvement in unblinded predictions was achieved by accounting for subject DM's valgus tibiofemoral alignment. This allowed the missing marker on the medial epicondyle to be virtually replaced more accurately. The resultant correction to the position of the tibiofemoral joint centre of rotation in the dynamic trials positively influenced the lateral force prediction. In particular, in the smooth gait trial the overprediction of the second peak that was observed in the blinded predictions was removed. The subject-specific reductions of muscle strength decreased the muscle forces, resulting in lower tibiofemoral forces. This was most evident in the reduction of the RMSE and increase in R^2 in the medial compartment during both smooth and bouncy gait trials. Several musculoskeletal modelling studies have reported an improvement in tibiofemoral contact force estimations by implementing subject-specific anatomical geometry parameters [14,44]. The study of DeMers et al. [45] has reported that by prohibiting knee muscle activations tibiofemoral forces could be decreased from over to underestimation, especially in the second peak of a gait cycle. Similar to those findings, our study demonstrated that the predictions in the unblinded model were significantly improved when subject-specific input information was fully applied.

Hip joints with three rotational degrees of freedom are often used in lower limb musculoskeletal models [43, 44]. This study indicated that this simplification should be subject-dependent. The additional kinematic constraints on the hip joint did not substantially alter the loading predictions at the knee joint, especially for subjects with a normal hip joint (Table 6). This revealed that the addition of such constraints is

appropriate for subjects for whom the joint translations are measured to be negligible, or for whom joint translation are simply not possible, for example in a constrained hip joint replacement, or in a reverse shoulder prosthesis. We do not propose adding such a constraint for other cases as hip joint distraction can, in some cases, be present in gait and other motions [46, 47].

Our third aim was to evaluate the performance of our subject-specific musculoskeletal model for a wider range of ADLs. Normal gait predictions showed similar error ranges to those obtained from smooth and bouncy gait trials with RMSEs for total tibiofemoral force of between 0.48 and 0.65 times BW (Table 4). The forces during squatting (0.46 to 1.01 times BW) and sit-to-stand (0.70 to 0.99 times BW) were overestimated when compared with the measured tibiofemoral contact forces, with RMSE for the total force between 0.46 and 1.01 times BW (Table 4). These results were consistent with the results from the conventional joint-based musculoskeletal modelling simulations, which reported peak forces of up to 3.9 times BW for gait and forces in the range of 2.4 to 4.9 times BW or even higher during other ADLs [9,48-50]. As the segment-based model can predict tibiofemoral force patterns with an average R^2 value of 0.77 and the errors in the tibiofemoral forces show comparable magnitudes, the presented modelling approach provides a new possibility for studying the mechanical function of the musculoskeletal system.

This study has a number of limitations. Firstly, each subject's PCSAs were identical to those determined in a generic dataset based on a cadaver dissection [27]. The study of Handsfield et al. [51] had shown that muscle volumes obtained from

cadavers did not match well to muscle volumes collected in vivo which would have an important influence on the maximum potential muscle forces presented. An appropriate scaling through the muscle PCSAs should be incorporated in the model in order to better account for the anatomical variability. Second, discrepancies in the timing of muscle active states compared to the EMG signal were observed from several predicted muscles forces. As muscle activation patterns of patients following total knee arthroplasty may not coincide with activation patterns of healthy patients [43], the cost function minimising the sum of cubed muscle stresses may not be appropriate for all subjects. Errors of up to 1.82 times BW were obtained for predictions of the second peak value of tibiofemoral articular contact force during normal gait. This would limit the model's clinical applicability in, for example, predicting the wear of joint replacements, where the absolute values of load are key. In DeMers et al. [45] similar over-predictions were found when using an objective function minimising the sum of squared muscle activations; these peaks can be reduced by changing the objective function. Incorporating the EMG data quantitatively in the optimization stage seems to be able to better predict muscle activation patterns for symptomatic subjects and hence further improve the tibiofemoral force estimations [14]. Third, as the ligaments' attachment sites could not be determined accurately from the subjects' CT scans, they were excluded in our subject-specific anatomical model. Ligaments play an important role in maintaining the stability of the knee joint [44]; therefore, including ligament models in the future would be beneficial for understanding the interaction mechanism

between the muscle forces, ligament forces and artificial contact forces around the knee.

CONCLUSIONS

In conclusion, this study shows that taking patient-specific geometry data, strength data, kinematic and kinetic data as the input to a segment-based musculoskeletal model, contact forces can be estimated for gait and other ADLs such as squatting and sit-to-stand. From the comparison between blinded and unblinded results, the segment-based musculoskeletal model was identified to be sensitive to a number of factors: the patient-specific anatomical geometry, such as varus/valgus leg alignment and medio-lateral contact points; maximum allowable muscle forces; and marker trajectories in the static and dynamic trials. As segment-based musculoskeletal modelling can predict muscle and joint forces as accurately as conventional joint-based musculoskeletal simulations it provides a new opportunity to study the mechanical function of the musculoskeletal system.

FUNDING

This research was supported by the Medical Engineering Solutions in Osteoarthritis Centre of Excellence at Imperial College London, which is funded by the Wellcome Trust and the Engineering and Physical Sciences Research Council (EPSRC). AEK was supported by the Imperial College London Junior Research Fellowship Scheme.

NOMENCLATURE

2

AdB	Adductor brevis
ADL	Activity of daily living
BW	Body weight
BF	Biceps femoris long head
CT	Computed tomography
EMG	Electromyography
GasMed	Gastrocnemius medialis
GMax	Gluteus maximus
Gra	Gracilis
MRI	Magnetic resonance imaging
PCSA	Physiological cross sectional area
R^2	Coefficient of determination
RF	Rectus femoris
RMSE	Root mean squared error
Sar	Sartorius
SemM	Semimembranosus
Sol	Soleus

TibA	Tibialis anterior
VasMed	Vastus medialis
VasLat	Vastus lateralis

REFERENCES

[1] Crowninshield, R.D., and Brand, R. A., 1981, "A Physiologically Based Criterion of Muscle Force Prediction in Locomotion," J. Biomech., **14**(11), pp. 793-801. DOI: 10.1016/0021-9290(81)90035-X

[2] Bull,A.M., Reilly, P., Wallace, A. L., Amis, A. A., and Emery, R. J., 2005, "A Novel Technique to Measure Active Tendon Forces: Application to the Subscapularis Tendon," Knee. Surg. Sports. Traumatol. Arthrosc., **13**(2), pp. 145-150. DOI: 10.1007/s00167-004-0556-y

[3] Bergmann,G., Graichen, F., and Rohlmann, A., 1993, "Hip Joint Loading During Walking and Running, Measured in Two Patients," J. Biomech., **26**(8), pp. 969-990. DOI: 10.1016/0021-9290(93)90058-M

[4] Knarr,B.A., and Higginson, J. S., 2015, "Practical Approach to Subject-Specific Estimation of Knee Joint Contact Force," J. Biomech., **48**(11), pp. 2897-2902. DOI: 10.1016/j.jbiomech.2015.04.020

[5] Kinney,A.L., Besier, T. F., Silder, A., Delp, S. L., D'Lima, D. D., and Fregly, B. J., 2013, "Changes in In Vivo Knee Contact Forces Through Gait Modification," J. Orthop. Res., **31**(3), pp. 434-440. DOI: 10.1002/jor.22240

[6] Modenese,L., Phillips, A. T., and Bull, A. M., 2011, "An Open Source Lower Limb Model: Hip Joint Validation," J. Biomech., **44**(12), pp. 2185-2193. DOI: 10.1016/j.jbiomech.2011.06.019

[7] Guess,T.M., Stylianou, A. P., and Kia, M., 2014, "Concurrent Prediction of Muscle and Tibiofemoral Contact Forces During Treadmill Gait," J. Biomech. Eng., **136**(2), p.021032. DOI: 10.1115/1.4026359

[8] Nikooyan,A.A., Veeger, H. E., Westerhoff, P., Graichen, F., Bergmann, G., and van der Helm, F. C., 2010, "Validation of the Delft Shoulder and Elbow Model Using In-Vivo Glenohumeral Joint Contact Forces," J. Biomech., **43**(15), pp. 3007-3014. DOI: 10.1016/j.jbiomech.2010.06.015

[9] Mizu-Uchi,H., Colwell, C. W., Jr., Flores-Hernandez, C., Fregly, B. J., Matsuda, S., and D'Lima, D. D., 2015, "Patient-Specific Computer Model of Dynamic Squatting After Total Knee Arthroplasty," J. Arthroplasty., **30**(5), pp. 870-874. DOI: 10.1016/j.arth.2014.12.021

[10] Stylianou,A.P., Guess, T. M., and Kia, M., 2013, "Multibody Muscle Driven Model of an Instrumented Prosthetic Knee During Squat and Toe Rise Motions," J. Biomech. Eng., **135**(4), p. 041008. DOI: 10.1115/1.4023982

[11] Fregly,B.J., Besier, T. F., Lloyd, D. G., Delp, S. L., Banks, S. A., Pandy, M. G., and D'Lima, D. D., 2012, "Grand Challenge Competition to Predict In Vivo Knee Loads," J. Orthop. Res., **30**(4), pp. 503-513. DOI: 10.1002/jor.22023

[12] Arnold,E.M., Ward, S. R., Lieber, R. L., and Delp, S. L., 2010, "A Model of the Lower Limb for Analysis of Human Movement," Ann. Biomed. Eng., **38**(2), pp. 269-279. DOI: 10.1007/s10439-009-9852-5

[13] Donnelly,C.J., Lloyd, D. G., Elliott, B. C., and Reinbolt, J. A., 2012, "Optimizing Whole-Body Kinematics to Minimize Valgus Knee Loading During Sidestepping: Implications for ACL Injury Risk," J. Biomech., **45**(8), pp. 1491-1497. DOI: 10.1016/j.jbiomech.2012.02.010

[14] Gerus,P., Sartori, M., Besier, T. F., Fregly, B. J., Delp, S. L., Banks, S. A., Pandy, M. G., D'Lima, D. D., and Lloyd, D. G., 2013, "Subject-Specific Knee Joint Geometry Improves Predictions of Medial Tibiofemoral Contact Forces," J. Biomech., **46**(16), pp. 2778-2786. DOI: 10.1016/j.jbiomech.2013.09.005

[15] Uvehammer,J., Karrholm, J., and Brandsson, S., 2000, "In Vivo Kinematics of Total Knee Arthroplasty. Concave Versus Posterior-Stabilised Tibial Joint Surface," J. Bone. Joint. Surg. Br., **82**(4), pp. 499-505. DOI: 10.1054/arth.2001.17939

[16] Cleather,D.J., and Bull, A. M. J., 2015, "The Development of a Segment-based Musculoskeletal Model of the Lower Limb: Introducing FreeBody," Royal Society Open Science., **2**(6), DOI: 10.1098/rsos.140449

[17] Dumas,R., Aissaoui, R., and de Guise, J. A., 2004, "A 3D Generic Inverse Dynamic Method Using Wrench Notation and Quaternion Algebra," Comput. Methods. Biomech. Biomed. Engin., **7**(3), pp. 159-166. DOI: 10.1080/10255840410001727805

[18] Cleather,D.J., and Bull, A. M., 2011, "An Optimization-based Simultaneous Approach to the Determination of Muscular, Ligamentous, and Joint Contact Forces Provides Insight into Musculoligamentous Interaction," Ann. Biomed. Eng., **39**(7), pp. 1925-1934. DOI: 10.1007/s10439-011-0303-8

[19] Cleather,D.J., Goodwin, J. E., and Bull, A. M., 2011, "An Optimization Approach to Inverse Dynamics Provides Insight as to the Function of the Biarticular Muscles During Vertical Jumping," Ann. Biomed. Eng., **39**(1), pp. 147-160. DOI: 10.1007/s10439-010-0161-9

[20] Kirking,B., Krevolin, J., Townsend, C., Colwell, C. W., Jr., and D'Lima, D. D., 2006, "A Multiaxial Force-Sensing Implantable Tibial Prosthesis," J. Biomech., **39**(9), pp. 1744-1751. DOI: 10.1016/j.jbiomech.2005.05.023

[21] Kinney, A. L., Besier, T. F., D'Lima, D. D., and Fregly, B. J., 2014, "Update on Grand Challenge Competition to Predict In Vivo Knee Loads," J. Biomech. Eng., **135**(2), p. 021012. DOI: 10.1115/1.4023255

[22] Anderson,F.C., and Pandy, M. G., 2001, "Dynamic Optimization of Human Walking," J. Biomech. Eng., **123**(5), pp. 381-390. DOI: 10.1115/1.1392310

[23] Damsgaard,M., Rasmussen, J., Christensen, S. T., Surma, E., and de Zee, M., 2006, "Analysis of Musculoskeletal Systems in the AnyBody Modeling System," Simul. Model. Pract. Theory., **14**(8), pp. 1100-1111. DOI: 10.1016/j.simpat.2006.09.001

[24] Delp,S.L., Anderson, F. C., Arnold, A. S., Loan, P., Habib, A., John, C. T., Guendelman, E., and Thelen, D. G., 2007, "OpenSim: Open-Source Software to Create and Analyze Dynamic Simulations of Movement," IEEE Trans. Biomed. Eng., **54**(11), pp. 1940-1950. DOI: 10.1109/TBME.2007.901024

[25] Cleather,D.J., and Bull, A. M., 2010, "Influence of Inverse Dynamics Methods on the Calculation of Inter-Segmental Moments in Vertical Jumping and Weightlifting," Biomed. Eng. Online.,**9** (74). DOI: 10.1186/1475-925X-9-74

[26] Dumas,R., Moissenet, F., Gasparutto, X., and Cheze, L., 2012, "Influence of Joint Models on Lower-Limb Musculo-Tendon Forces and Three-Dimensional Joint Reaction Forces During Gait," Proc. Inst. Mech. Eng H., **226**(2), pp. 146-160.

[27] Klein Horsman,M.D., Koopman, H. F., van der Helm, F. C., Prose, L. P., and Veeger, H. E., 2007, "Morphological Muscle and Joint Parameters for Musculoskeletal Modelling of the Lower Extremity," Clin. Biomech., **22**(2), pp. 239-247. DOI: 10.1016/j.clinbiomech.2006.10.003

[28] Yamaguchi, G.T., 2001. *Dynamic Modeling of Musculoskeletal Motion: A Vectorized Approach for Biomechanical Analysis in Three Dimensions*, New York: Springer, ISBN: 978-0-387-28750-8.

[29] Soderkvist,I., and Wedin, P. A., 1993, "Determining the Movements of the Skeleton Using Well-Configured Markers," J. Biomech., **26**(12), pp. 1473-1477.

[30] Kim Y.H., Park W.M., and Phuong B.T.T., 2010, "Effect of Joint Center Location on In-Vivo Joint Contact Forces During Walking", *Proc. ASME 2010 Summer Bioengineering Conference*, Naples, Florida, USA. DOI: 10.1115/SBC2010-19353

[31] Hast M.W., and Piazza S.J., 2013. "Dual-Joint Modeling for Estimation of Total Knee Replacement Contact Forces During Locomotion," J. Biomech. Eng., **135**(2), p.021013. DOI: 10.1115/1.4023320

[32] Manal K., and Buchanan T.S., 2012. "Predictions of Condylar Contact During Normal and Medial Thrust Gait," *Proc. ASME 2012 Summer Bioengineering Conference*, Fajardo, Puerto Rico, USA. DOI: 10.1115/SBC2012-80560

[33] Knowlton C.B., Wimmer M.A., and Lundberg H.J., 2012. "Grand Challenge Competition: A Parametric Numerical Model to Predict In Vivo Medial and Lateral Knee Forces in Walking Gaits," *Proc. ASME 2012 Summer Bioengineering Conference,* Fajardo, Puerto Rico, USA. DOI: 10.1115/SBC2012-80581

[34] Thelen,D.G., Won, C. K., and Schmitz, A. M., 2014, "Co-Simulation of Neuromuscular Dynamics and Knee Mechanics During Human Walking," J. Biomech. Eng., **136**(2), p. 021033. DOI: 10.1115/1.4026358

[35] Chen,Z., Zhang, X., Ardestani, M. M., Wang, L., Liu, Y., Lian, Q., He, J., Li, D., and Jin, Z., 2014, "Prediction of In Vivo Joint Mechanics of an Artificial Knee Implant Using Rigid Multi-Body Dynamics with Elastic Contacts," Proc. Inst. Mech. Eng H., **228**(6), pp. 564-575. DOI: 10.1177/0954411914537476

[36] Southgate,D.F., Cleather, D. J., Weinert-Aplin, R. A., and Bull, A. M., 2012, "The Sensitivity of a Lower Limb Model to Axial Rotation Offsets and Muscle Bounds at the Knee," Proc. Inst. Mech. Eng H., **226**(9), pp. 660-669. DOI: 10.1177/0954411912439284

[37] Narici,M.V., and Maganaris, C. N., 2006, "Adaptability of Elderly Human Muscles and Tendons to Increased Loading," J. Anat., **208**(4), pp. 433-443. DOI: 10.1111/j.1469-7580.2006.00548.x

[38] Samuel,D., and Rowe, P. J., 2009, "Effect of Ageing on Isometric Strength Through Joint Range at Knee and Hip Joints in Three Age Groups of Older Adults," Gerontology., **55**(6), pp. 621-629. DOI: 10.1159/000236043

[39] D'Lima,D.D., Townsend, C. P., Arms, S. W., Morris, B. A., and Colwell, C. W., Jr., 2005, "An Implantable Telemetry Device to Measure Intra-Articular Tibial Forces," J. Biomech., **38**(2), pp. 299-304. DOI: 10.1016/j.jbiomech.2004.02.011

[40] Silva,M., Shepherd, E. F., Jackson, W. O., Pratt, J. A., McClung, C. D., and Schmalzried, T. P., 2003, "Knee Strength after Total Knee Arthroplasty," J Arthroplasty., **18**(5), pp. 605-611. DOI: 10.1016/S0883-5403(03)00191-8

[41] Arnold, E. M., Hamner, S. R., Seth, A., Millard, M., & Delp, S. L.,2013, “How Muscle Fiber Lengths and Velocities Affect Muscle Force Generation as Humans Walk and Run at Different Speeds.” J.Exp.Biol., **216**(11), pp. 2150–60. DOI:10.1242/jeb.075697.

[42] Giroux, M., Moissenet, F., & Dumas, R.,2013 “EMG-based Validation of Musculo-

Skeletal Models for Gait Analysis." Comput. Methods Biomech. Biomed. Engin., **16**(5), pp. 152–54. DOI:10.1080/10255842.2013.815878.

[43] Moissenet,F., Cheze, L., and Dumas, R., 2014, "A 3D Lower Limb Musculoskeletal Model for Simultaneous Estimation of Musculo-Tendon, Joint Contact, Ligament and Bone Forces During Gait," J. Biomech., **47**(1), pp. 50-58. DOI: 10.1016/j.jbiomech.2013.10.015

[44] Marra,M.A., Vanheule, V., Fluit, R., Koopman, B. H., Rasmussen, J., Verdonschot, N., and Andersen, M. S., 2015, "A Subject-Specific Musculoskeletal Modeling Framework to Predict In Vivo Mechanics of Total Knee Arthroplasty," J. Biomech. Eng., **137**(2), p. 020904. DOI: 10.1115/1.4029258

[45] DeMers, M. S., Pal, S., and Delp, S. L.. 2014. "Changes in Tibiofemoral Forces due to Variations in Muscle Activity During Walking." J. Orthop. Res., **32** (6), pp. 769–76. DOI:10.1002/jor.22601.

[46] Akiyama, K., Sakai, T., Koyanagi, J., Yoshikawa, H., and Sugamoto, K.,2011. "Evaluation of Translation in the Normal and Dysplastic Hip Using Three-Dimensional Magnetic Resonance Imaging and Voxel-based Registration. " OSIRIS., **19**(6), pp. 700–710. DOI:10.1016/j.joca.2011.01.017

[47] Gilles, B., Christophe, F. K., Magnenat-Thalmann, N., Becker, C. D., Duc, S. R., Menetrey, J., and Hoffmeyer, P.,2009. "MRI-based Assessment of Hip Joint Translations, " J. Biomech., **42**(9), pp. 1201–1205. DOI:10.1016/j.jbiomech.2009.03.033

[48] Shelburne,K.B., and Pandy, M. G., 2002, "A Dynamic Model of the Knee and Lower Limb for Simulating Rising Movements," Comput. Methods Biomech. Biomed. Engin., **5**(2), pp. 149-159. DOI: 10.1080/10255840290010265

[49] Smith,S.M., Cockburn, R. A., Hemmerich, A., Li, R. M., and Wyss, U. P., 2008, "Tibiofemoral Joint Contact Forces and Knee Kinematics During Squatting," Gait Posture., **27**(3), pp. 376-386. DOI: 10.1016/j.gaitpost.2007.05.004

[50] Dahlkvist,N.J., Mayo, P., and Seedhom, B. B., 1982, "Forces During Squatting and Rising From a Deep Squat," Eng. Med., **11**(2), pp. 69-76. DOI: 10.1243/EMED_JOUR_1982_011_019_02

[51] Handsfield, G. G., Meyer, C. H., Hart, J. M., Abel, M. F., and Blemker, S. S. 2014, " Relationships of 35 Lower Limb Muscles to Height and Body Mass Quantified Using MRI", J. Biomech., **47**(3), pp. 631–638. DOI:10.1016/j.jbiomech.2013.12.002.

Figure Captions List

2

Fig. 1 Blinded model predictions of medial, lateral and total tibiofemoral contact forces compared with in vivo measurements obtained during two different gait trials

Fig. 2 Unblinded model predictions of medial, lateral and total tibiofemoral contact forces compared with in vivo measurements obtained during two different gait trials

Fig.3 Comparison of the predicted muscle forces in blinded and unblinded models and the corresponding active/inactive state for muscles of adductor brevis (AdB), gluteus maximus (GMax), gracilis (Gra), semimembranosus (SemM), biceps femoris long head (BF), vastus medialis (VasMed), vastus lateralis (VasLat), rectus femoris (RF), gastrocnemius medialis (GasMed), sartorius (Sar), tibialis anterior (TibA) and soleus (Sol)

Table Caption List

2

Table 1 Comparison between in vivo and blinded predictions of tibiofemoral contact forces during a single gait cycle for two gait trials

Table 2 Peak isometric extension and flexion torques for subjects with total knee arthroplasty and matched controls from Silva et al. [34] and those for subjects JW and DM

Table 3 Comparison between in vivo and predicted tibiofemoral contact forces during a single gait cycle for smooth1 and bouncy5 gait trials following model modification

Table 4 Comparison between in vivo and predicted tibiofemoral contact forces during normal gait, squatting, and sit-to-stand trials averaged for each subject over all trials

Table 5 Comparison between predicted and measured peak forces in the tibiofemoral joint in normal gait, squatting, and sit-to-stand trials averaged for each subject over all trials

Table 6 Comparison between predicted and measured tibiofemoral contact forces in smooth, bouncy and normal gait trials for 3 subjects

4

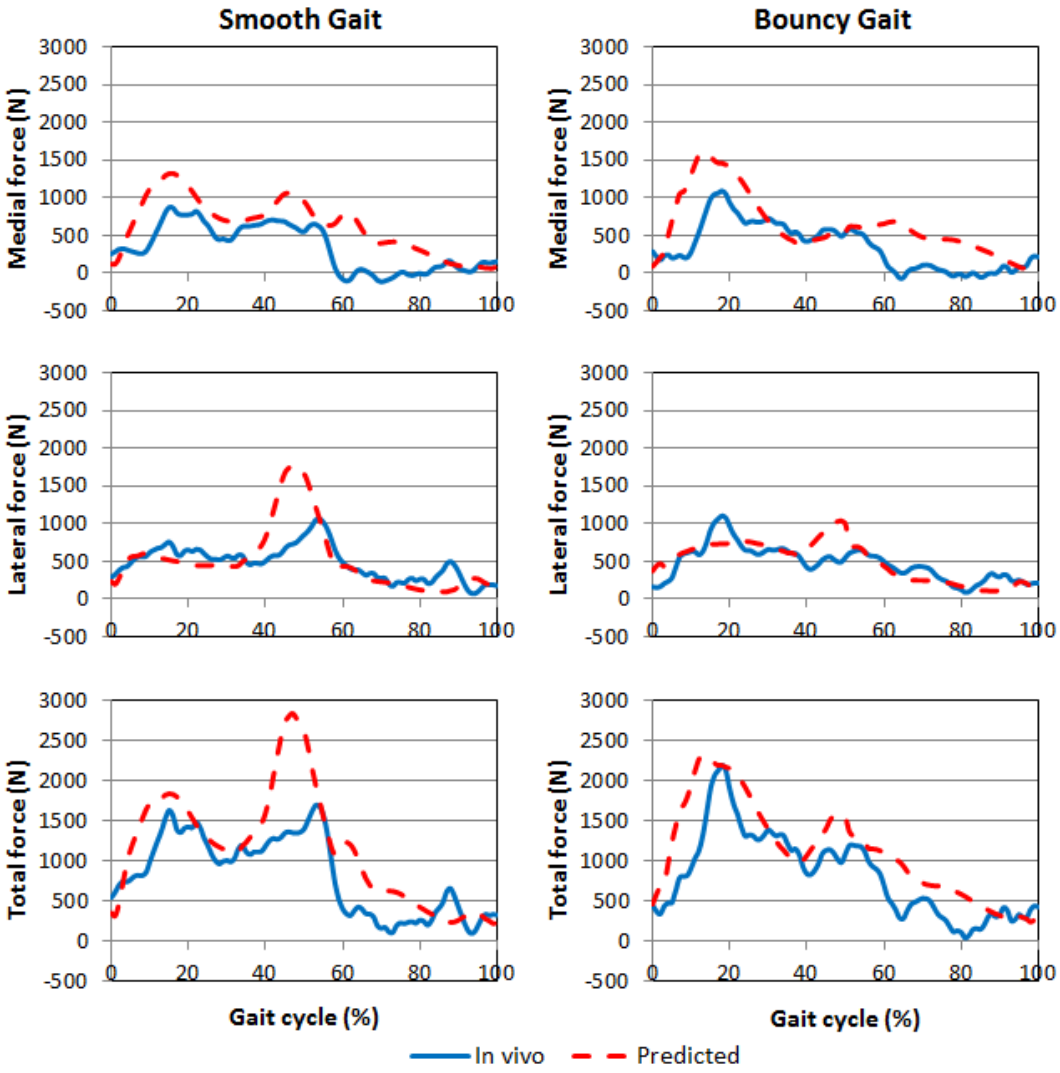

Fig. 1 Blinded model predictions of medial, lateral and total tibiofemoral contact forces compared with in vivo measurements obtained during two different gait trials

Table 1. Comparison between in vivo and blinded predictions of tibiofemoral contact forces during a single gait cycle for two gait trials

Gait Trial	Medial		Lateral		Total	
	RMSE (N)	R^2	RMSE (N)	R^2	RMSE (N)	R^2
Smooth1	383	0.56	315	0.50	526	0.69
Bouncy5	413	0.44	186	0.53	427	0.74

Table 2. Peak isometric extension and flexion torques for subjects with total knee arthroplasty and matched controls from Silva et al. [40] and those for subjects JW and DM

	Isometric extension peak torque (N▪m)	Isometric flexion peak torque (N▪m)
Control subjects	113	50
Total knee arthroplasty	92	31
JW	96	51
DM	79	25

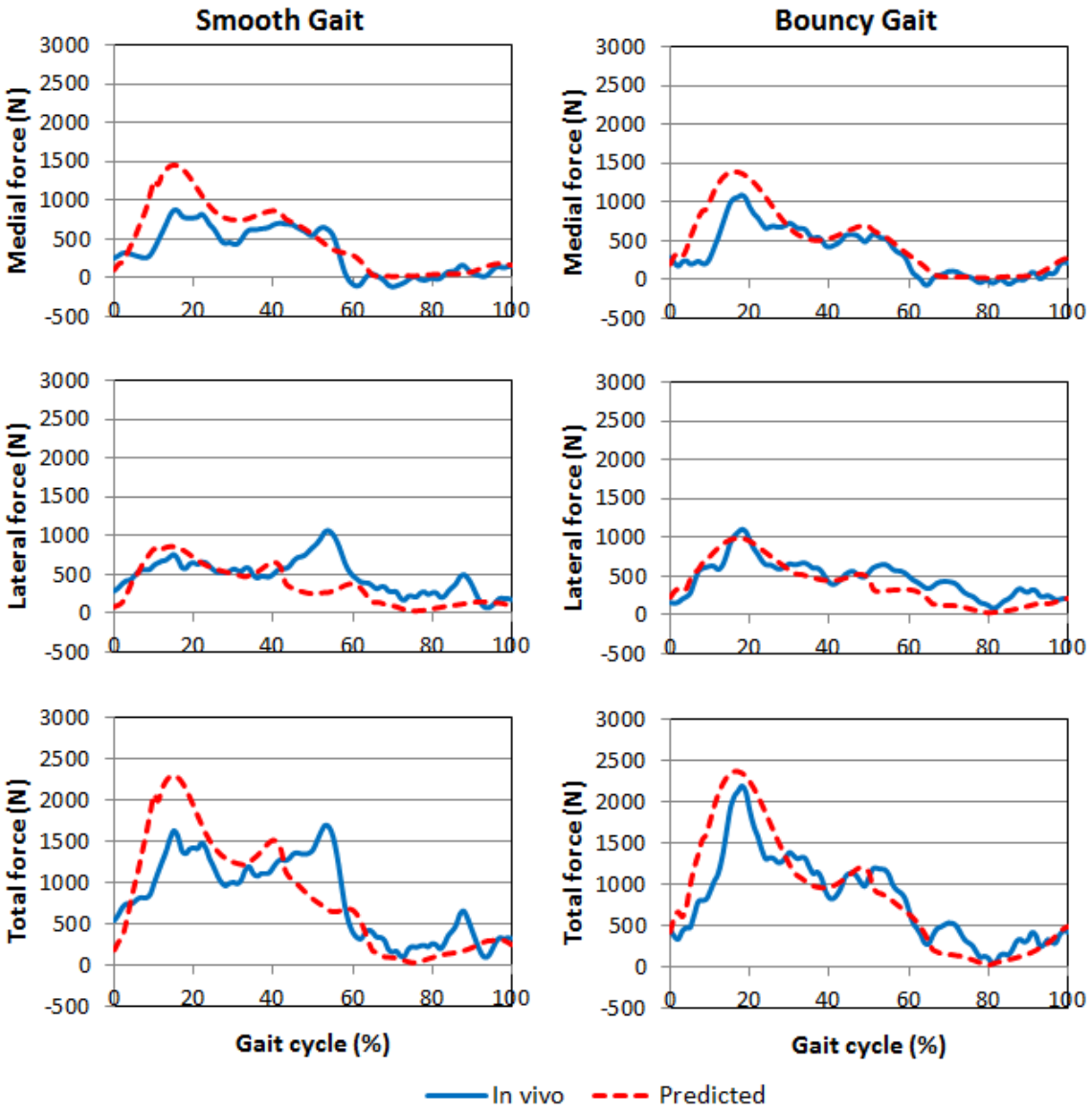

2 Fig. 2 Unblinded model predictions of medial, lateral and total tibiofemoral contact forces compared with in vivo measurements obtained during two different gait trials

4

Table 3. Comparison between in vivo and predicted tibiofemoral contact forces during a single gait cycle for smooth1 and bouncy5 gait trials following model modification

	Medial		Lateral		Total	
	RMSE (N)	R^2	RMSE (N)	R^2	RMSE (N)	R^2
Smooth1	287	0.75	262	0.31	429	0.62
Bouncy5	242	0.79	163	0.74	320	0.82

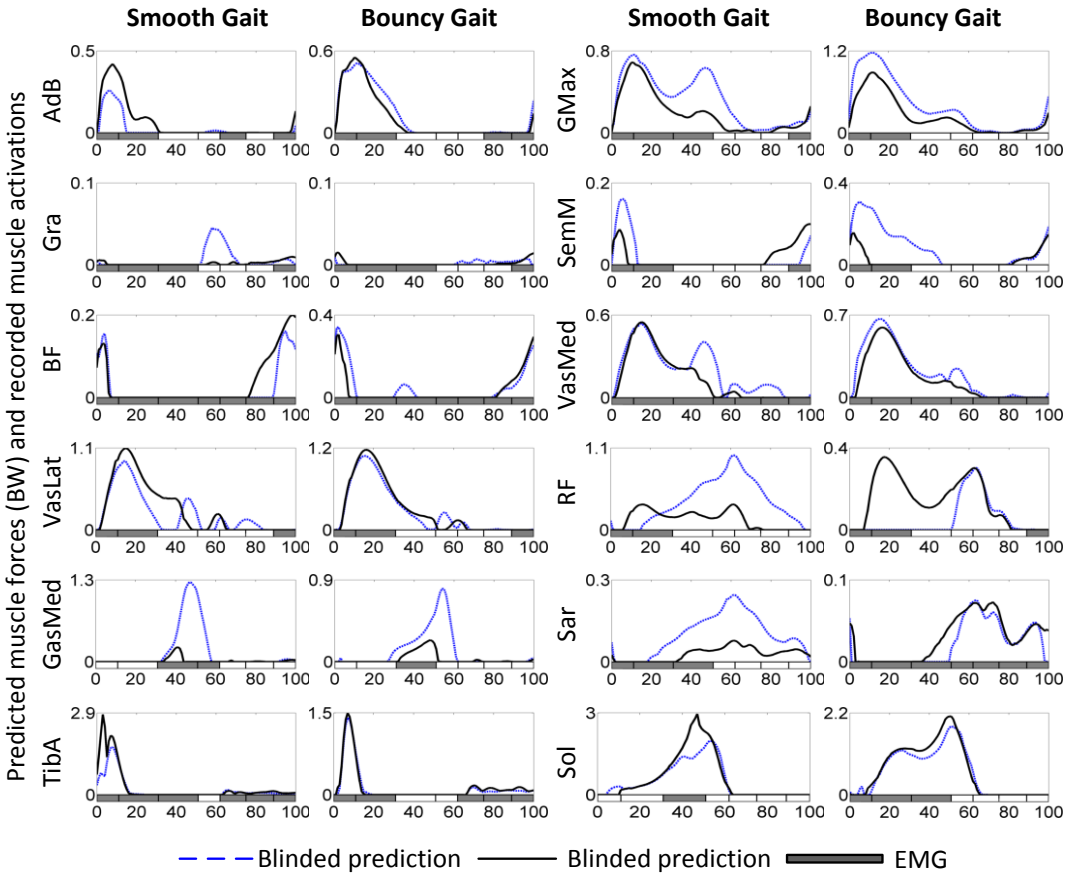

Fig. 3 Comparison of the predicted muscle forces in blinded and unblinded models and the corresponding active/inactive state for muscles of adductor brevis (AdB), gluteus maximus (GMax), gracilis (Gra), semimembranosus (SemM), biceps femoris long head (BF), vastus medialis (VasMed), vastus lateralis (VasLat), rectus femoris (RF), gastrocnemius medialis (GasMed), sartorius (Sar), tibialis anterior (TibA) and soleus (Sol).

Table 4. Comparison between in vivo and predicted tibiofemoral contact forces during normal gait, squatting, and sit-to-stand trials averaged for each subject over all trials

Task	Subject	Medial		Lateral		Total	
		RMSE (BW)	R^2	RMSE (BW)	R^2	RMSE (BW)	R^2
Normal gait	JW	0.252	0.844	0.469	0.516	0.653	0.538
	PS	0.480	0.719	0.274	0.301	0.491	0.727
	DM	0.506	0.798	0.460	0.278	0.484	0.748
Squat	JW	0.252	0.854	0.741	0.885	0.861	0.858
	PS	0.593	0.440	0.220	0.835	0.463	0.765
	DM	0.660	0.859	0.412	0.230	1.010	0.873
Sit-to-stand	JW	0.146	0.913	0.773	0.705	0.810	0.970
	PS	0.751	0.240	0.287	0.693	0.703	0.525
	DM	0.520	0.874	0.527	0.488	0.991	0.897

Table 5. Comparison between predicted and measured peak forces in the tibiofemoral joint in normal gait, squatting, and sit-to-stand trials averaged for each subject over all trials

Task	Subject	Peak	Mean difference in peak force (BW)		
			medial	lateral	total
Normal gait	JW	1st	-0.12	0.28	-0.29
		2nd	0.33	1.47	1.82
	PS	1st	-0.95	1.49	-0.5
		2nd	-0.78	3.41	0.23
	DM	1st	-0.71	-0.37	0.45
		2nd	0.23	-0.89	-0.72
Squat	JW		0.62	0.94	1.55
	PS		0.76	0.25	0.44
	DM		0.64	0.27	1.03
Sit-to-stand	JW	1st	0.34	0.97	1.02
		2nd	0.17	1.15	1.33
	PS	1st	2.00	0.85	1.91
		2nd	2.00	0.85	1.91
	DM	1st	0.50	0.61	1.10
		2nd	0.59	0.64	1.32

Table 6. Comparison between predicted and measured tibiofemoral contact forces in smooth, bouncy and normal gait trials for 3 subjects.

Subject	Trial	6DOFs hip model				3DOFs hip model			
		Medial		Lateral		Medial		Lateral	
		RMSE (N)	R^2	RMSE (N)	R^2	RMSE (N)	R^2	RMSE (N)	R^2
DM	Smooth gait	287	0.75	262	0.31	301	0.79	416	0.22
	Bouncy gait	242	0.79	163	0.74	243	0.79	159	0.75
	Normal gait	328	0.86	294	0.27	368	0.88	304	0.46
PS	Normal gait	341	0.80	152	0.60	386	0.79	174	0.36
JW	Normal gait	325	0.72	262	0.67	178	0.82	276	0.59